Contribution to the benchmark proposal of Hans Kuerten: LES of particle-laden channel flow.

Simulations of Christian Gobert, TU Munich

January 19, 2010

1 Overview and description of the simulations

This document contains statistics corresponding to the statistics presented in Marchioli *et al.* [1]. The statistics are shown in the same order as in Marchioli *et al.* [1]. The shown data shown is from Hans Kuerten's (TU Eindhoven, TUE) DNS, downloaded from `http://cfd.cineca.it/` and results from Christian Gobert and Michael Manhart (TU Munich, TUM). The latter results were obtained by DNS, LES and semi-DNS, i.e., a simulation on the LES grid without LES model. Table 1 gives some details on the simulations. Furthermore,

- all grids are streched grids, i.e., finer close to the wall than at the channel center. The grids are shown in figure 1
- for LES, the dynamic Lagrange Smagorinsky model proposed by Meneveau *et al.* [2] was implemented
- the (filtered) Navier–Stokes equations were discretized by a second order Finite-Volume method
- for time advancement of the fluid flow, a third order Runge–Kutta method was implemented
- the particle velocity was integrated in time using a 4th order adaptive linear-implicit Runge–Kutta scheme (Rosenbrock–Wanner scheme)
- interpolation of fluid velocity on particles' position is trilinear or fourth order. For fourth order interpolation close to the wall, a non-symmetric stencil (with respect to the particle position) was chosen, i.e., close to the wall, the interpolation is based on the three points which are nearest to the wall and the wall itself where $u = v = w = 0$
- in accordance with the simulations of Hans Kuerten, the particle statistics were averaged from $t^+ = 0$ to $t^+ = 16000$
- the instantaneuous particle distribution in the steady state was extracted at $t^+ = 20000$
- all particle-related quantities are plotted at the y^+-value that corresponds to the lower boundary of the corresponding bin, i.e., the statistics of particles in the wall-nearest layer are plotted at $y^+ = 0$. The binning was chosen in accordance with the benchmark requirements, i.e., a hyperbolic tangent function. The reader is reminded that the binning for sampling particle statistics does not coincide with the grid for the fluid flow.

Table 1: Overview on the simulations

label	number of grid points	distance of first grid point to the wall	interpolation of fluid velocity seen by particles
DNS	128^3 (benchmark resolution)	$y^+ = 1$	trilinear
fine DNS	256^3	$y^+ = 0.7$	n.a.(fluid statistics only)
LES trilin	64^3 (benchmark resolution)	$y^+ = 2$	trilinear
LES 4thO.	64^3 (benchmark resolution)	$y^+ = 2$	4th order
semi-DNS trilin	64^3 (benchmark resolution)	$y^+ = 2$	trilinear
semi-DNS 4thO.	64^3 (benchmark resolution)	$y^+ = 2$	4th order

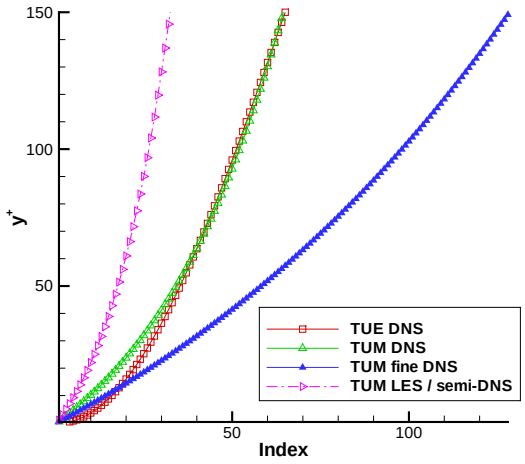

Figure 1: Grid spacing in the wall-normal direction

2 Some comments on the results

The following contains some comments on the results from sections 3 and 4.

2.1 Comments on the fluid statistics

Figures 2 to 6 show statistics on the fluid phase. Apparently the TUM DNS shows smaller rms values than the two reference DNS. This was to be expected because the TUM DNS is based on a second order Finite Volume scheme and shows therefore higher numerical dissipation that the UUD DNS and the TUE DNS which are both based on spectral methods. This hypothesis is supported by the fact that the TUM DNS on the fine grid is closer to the spectral solutions than the TUM DNS on the standard grid.
Concerning the LES result, it is remarkable that the dynamic Lagrangian Smagorinsky model leads to an overestimation of the mean velocity and rms of velocity fluctuations in the streamwise direction but an underestimation of the rms values in spanwise and wall-normal direction. However, this behavior is well known, see [2]. The results from the semi-DNS are as expected.
Concerning the streamwise/wall-normal component of the Reynolds stress, all DNS and even the semi-DNS agree very well with each other. The LES underpredicts that quantity (refering to its absolute value).
The shown fluid statistics are these which are presented in Marchioli *et al.* [1]. As requested by the benchmark specification, more statistics up to fourth order were computed. Concerning these statistics, good agreement between TUM DNS and TUE DNS was observed concerning second order statistics. Skewness and flatness seems to be predicted uncorrectly by TUM DNS, probably due to the low order of the scheme.

2.2 Comments on the particle statistics

Concerning particle statistics, Marchioli *et al.* [1] show the temporal development of particle concentration close to the wall. This quantity depends on the binning. It seems as if the binning is not the same in the TUE-simulations and the TUM simulations. However, figures 7 to 9 show the temporal development of particle concentration near the wall. In the TUM-simulations, this is the concentration below $y^+ = 0.36$ for $St = 1$ and $St = 5$. The $St = 25$-particles have a diameter of $0.765y^*$. Therefore these particles do not get closer to the wall than $y^+ = 0.38$. Consequently, figure 9 shows, concerning the TUM-simulations, the concentration below $y^+ = 0.73$ for $St = 25$. The TUE-simulations data was taken from the online repository.
Figures 7 to 9 show that in LES and semi-DNS, the particle concentration near the wall depends heavily on interpolation. For $St = 1$ and $St = 5$, fourth order interpolation leads to too low concentrations next to the wall in LES and semi-DNS, compared against the DNS result. However, this does not mean that LES or semi-DNS with fourth order interpolation does not predict turbophoresis, see below. The reader is reminded that for $St = 1$ and $St = 5$, figures 7 and 8 show the particles in $y^+ < 0.36$ whereas for $St = 25$, figure 9 shows the particles in $y^+ < 0.73$. Thus, figure 9 is not fully comparable to figures 7 and 8.
The particle concentration at the channel center is less dependent on binning. It is shown as a function of time in figures 10 to 12. The TUM DNS agrees well with the TUE DNS.

Figures 13 to 15 show the instantaneous particle concentrations in the statistically steady state (at $t^+ = 20000$). The leftmost point always refers to the concentration in $y^+ < 0.36$. It was already observed before that for $St = 1$ and $St = 5$, the fourth order interpolation leads to too low particle concentrations near the wall in LES or semi-DNS. Figures 13 and 14 show that actually fourth order interpolation leads to a shift of the concentration maximum towards the channel center. This shift cannot be observed with trilinear interpolation. Probably the shift is due to the asymmetry of the fourth order stencil near the wall. This issue might be clarified with Hans Kuerten's results which are based on a Hermite interpolation stencil close to the wall.
The mean streamwise particle velocites are shown in figures 16 to 18. The deviations of LES or semi-DNS to DNS are a consequence of the deviations observed for the fluid phase, cf. figure 2. The same holds for the rms values, figures 19 to 27.
The particle Reynolds stress differs significanly in DNS / LES or semi-DNS, cf. figures 28 to 30. This was not observed for the fluid Reynolds stress, cf. figure 6. The TUM DNS and the TUE DNS were in good agreement concerning the fluid Reynolds stress but concerning particle Reynolds stress, already these two DNS show different results. However, similar observations were already found by Marchioli *et al.* [1]. In that paper, several codes showed good agreement in fluid Reynolds stress but not so good agreement in particle Reynolds stress. In general, particle Reynolds stress seems to be underpredicted (refering to the absolute value) by LES or, even stronger, by semi-DNS.

3 Fluid statistics

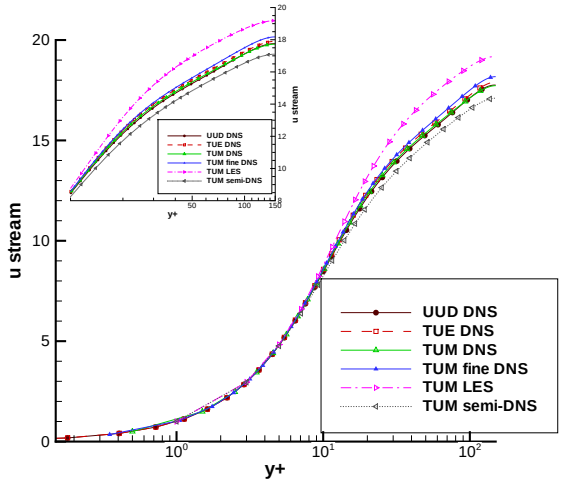

Figure 2: Mean streamwise fluid velocity

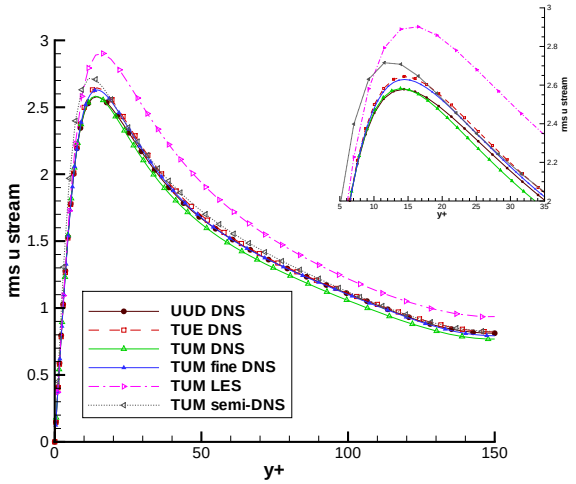

Figure 3: rms of fluid velocity fluctuations (streamwise)

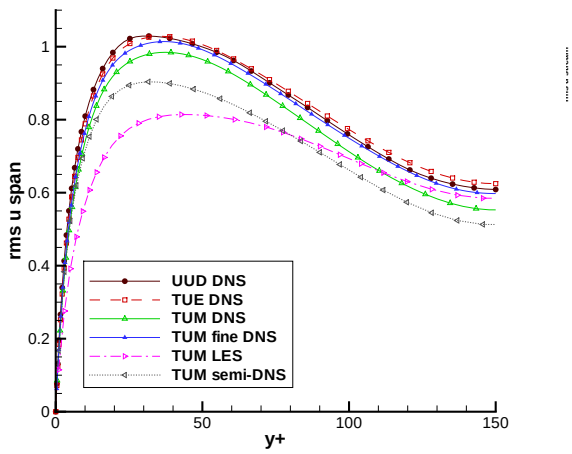

Figure 4: rms of fluid velocity fluctuations (spanwise)

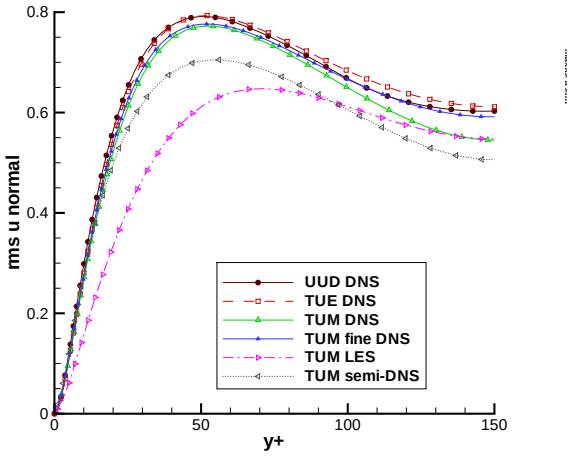

Figure 5: rms of fluid velocity fluctuations (wall-normal)

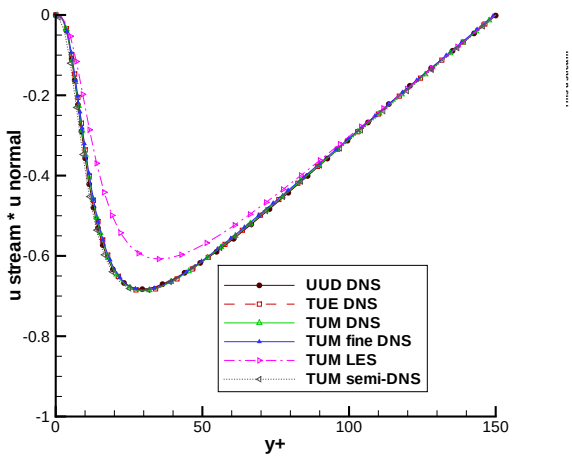

Figure 6: Fluid Reynolds stress: streamwise/wall-normal component

4 Particle statistics

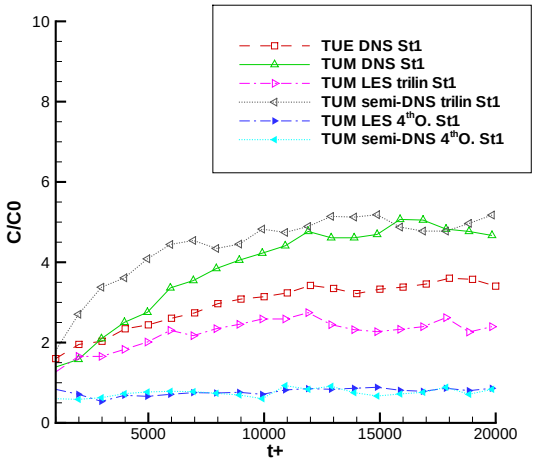

Figure 7: Particle concentration close to the wall (below $y^+ = 0.36$) as function of time, $St = 1$

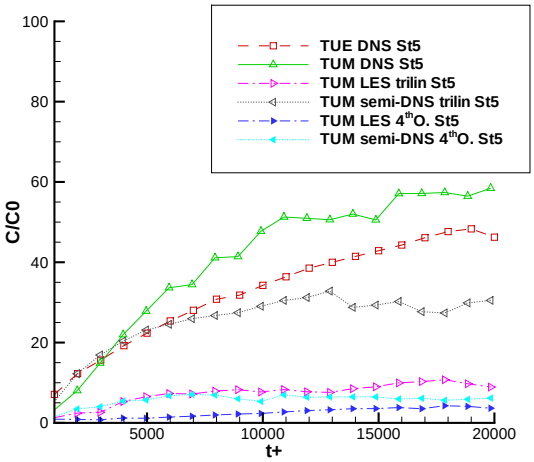

Figure 8: Particle concentration close to the wall (below $y^+ = 0.36$) as function of time, $St = 5$

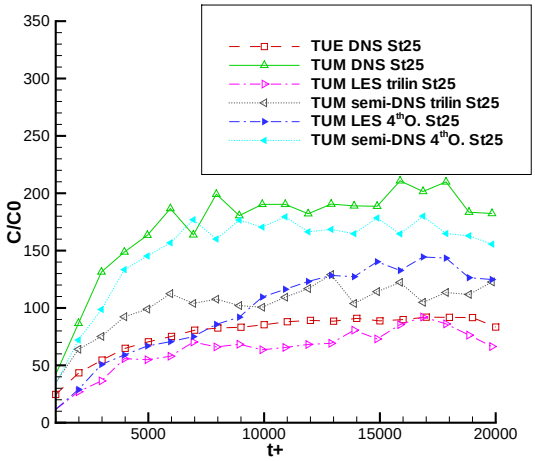

Figure 9: Particle concentration close to the wall (below $y^+ = 0.73$) as function of time, $St = 25$

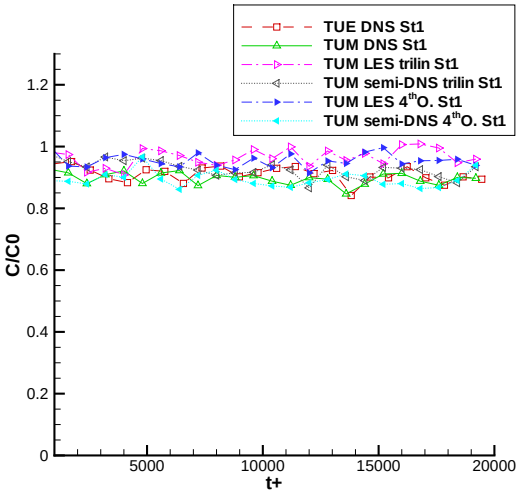

Figure 10: Particle concentration at the center as function of time, $St = 1$

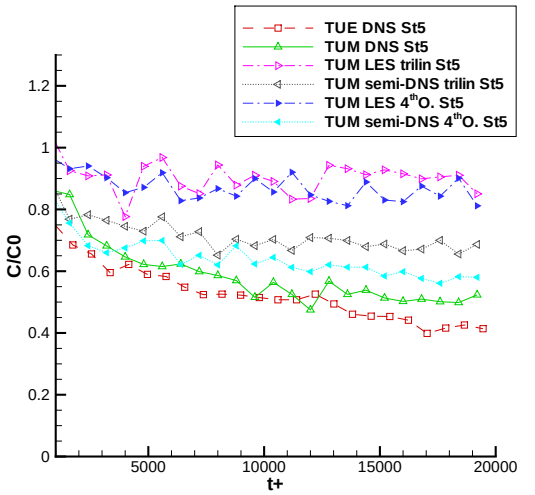

Figure 11: Particle concentration at the center as function of time, $St = 5$

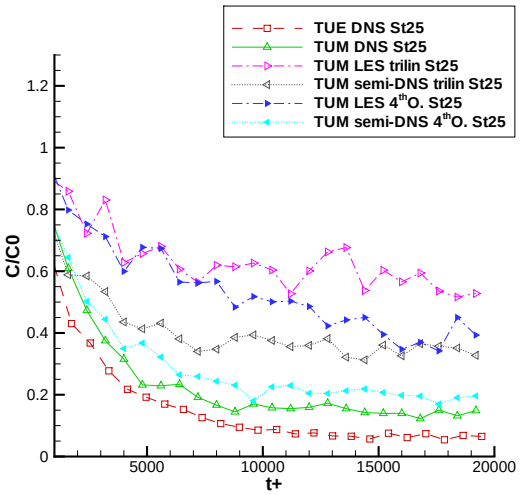

Figure 12: Particle concentration at the center as function of time, $St = 25$

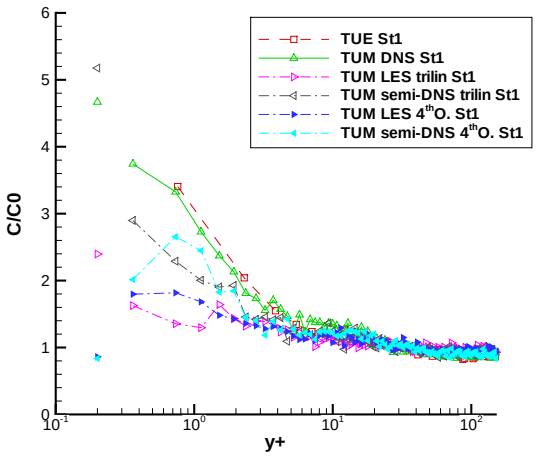

Figure 13: Instantaneous particle concentration profile at $t^+ = 20000$, $St = 1$. The leftmost point refers to the concentration in $y^+ < 0.36$.

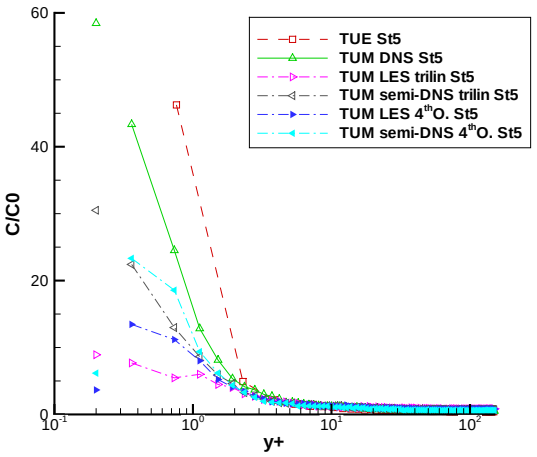

Figure 14: Instantaneous particle concentration profile at $t^+ = 20000$, $St = 5$. The leftmost point refers to the concentration in $y^+ < 0.36$.

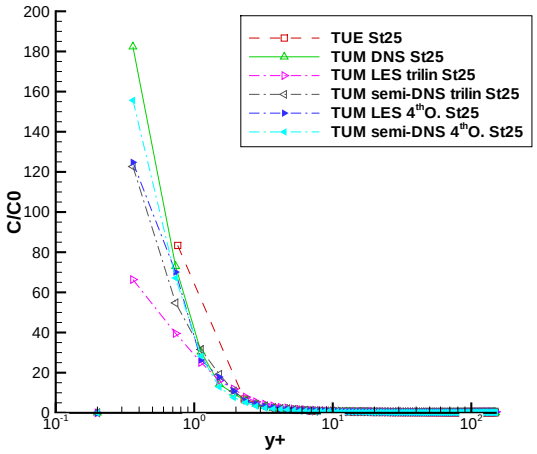

Figure 15: Instantaneous particle concentration profile at $t^+ = 20000$, $St = 25$. The leftmost point refers to the concentration in $y^+ < 0.36$.

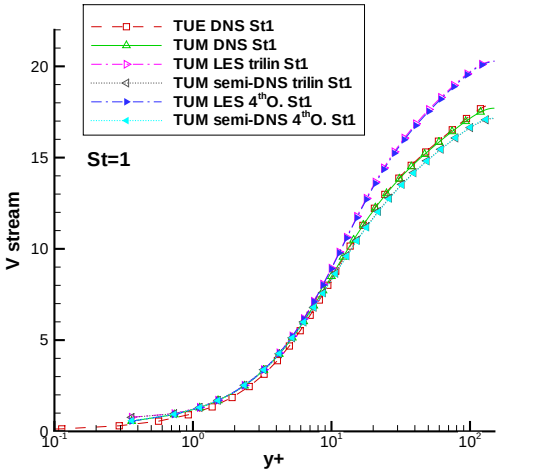

Figure 16: Mean streamwise particle velocity, $St = 1$

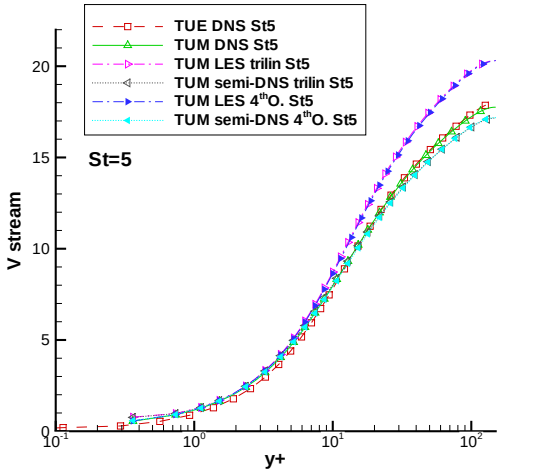

Figure 17: Mean streamwise particle velocity, $St = 5$

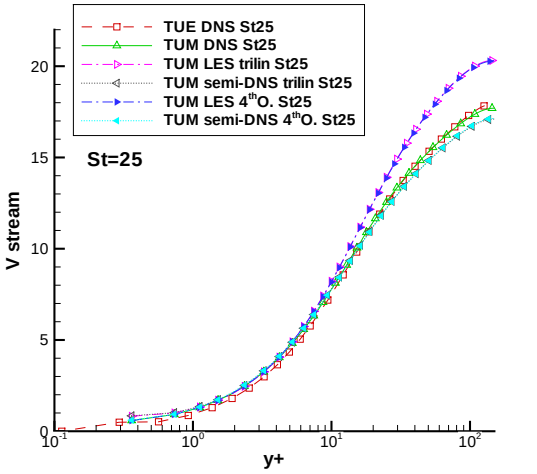

Figure 18: Mean streamwise particle velocity, $St = 25$

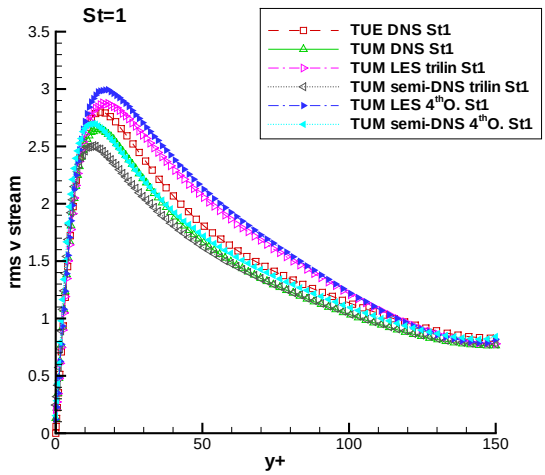

Figure 19: rms of particle streamwise velocity fluctuations, $St = 1$

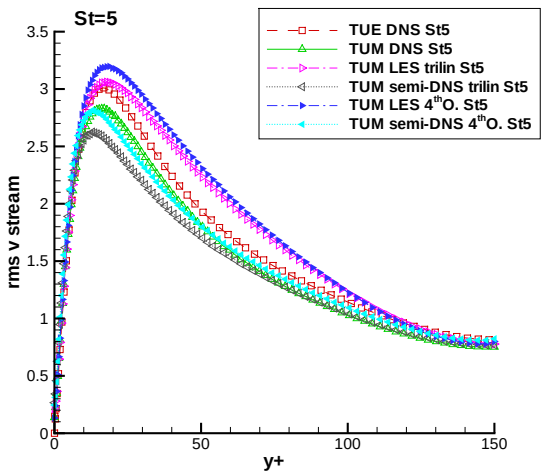

Figure 20: rms of particle streamwise velocity fluctuations, $St = 5$

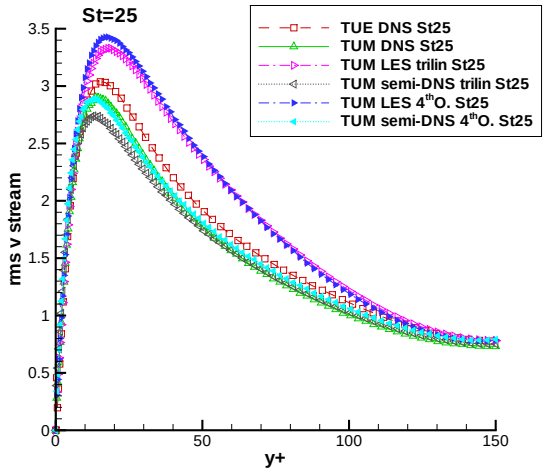

Figure 21: rms of particle streamwise velocity fluctuations, $St = 25$

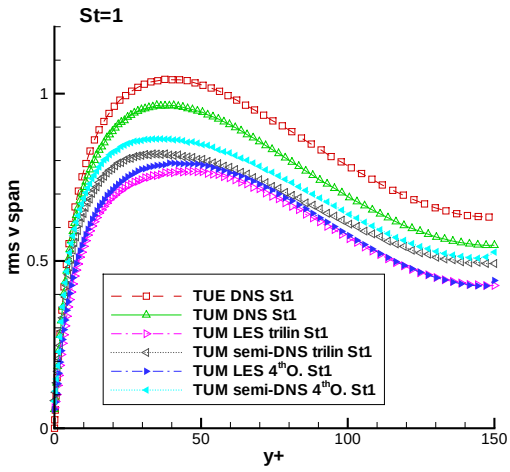

Figure 22: rms of particle spanwise velocity fluctuations, $St = 1$

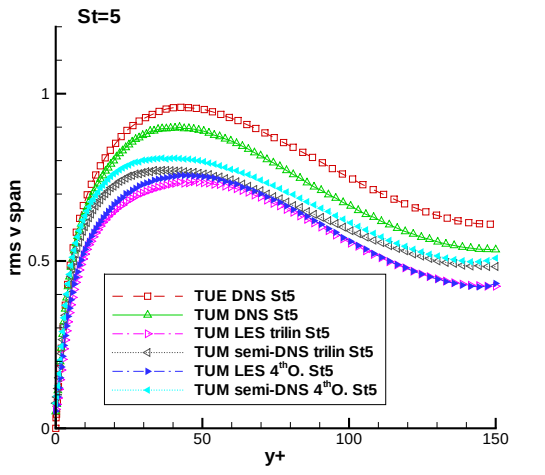

Figure 23: rms of particle spanwise velocity fluctuations, $St = 5$

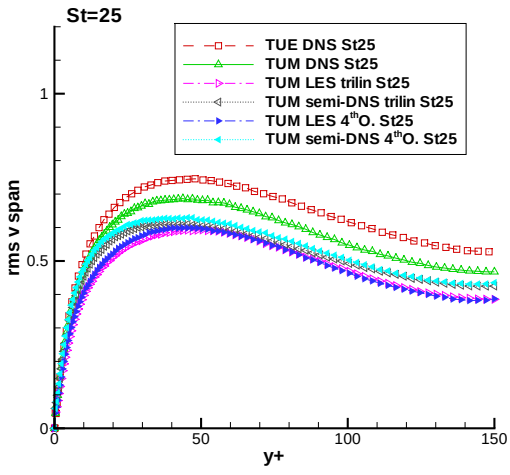

Figure 24: rms of particle spanwise velocity fluctuations, $St = 25$

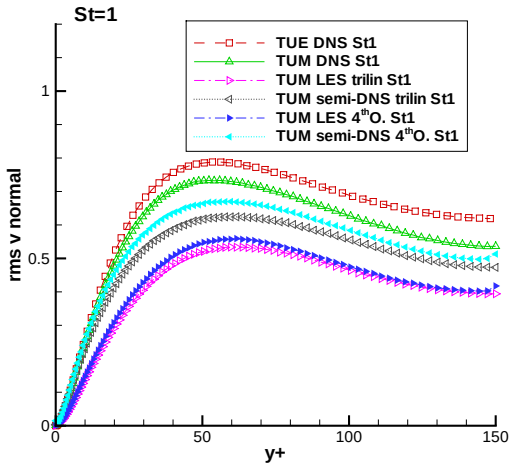

Figure 25: rms of particle wall-normal velocity fluctuations, $St = 1$

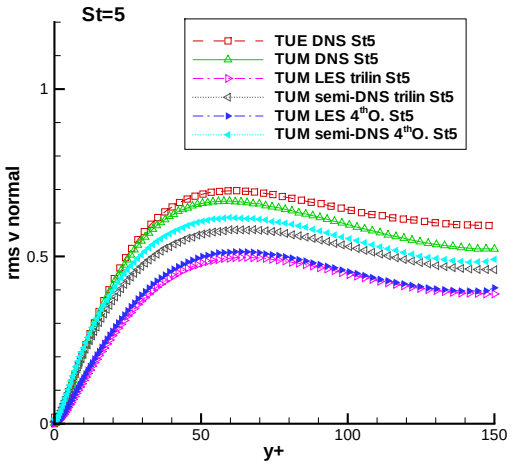

Figure 26: rms of particle wall-normal velocity fluctuations, $St = 5$

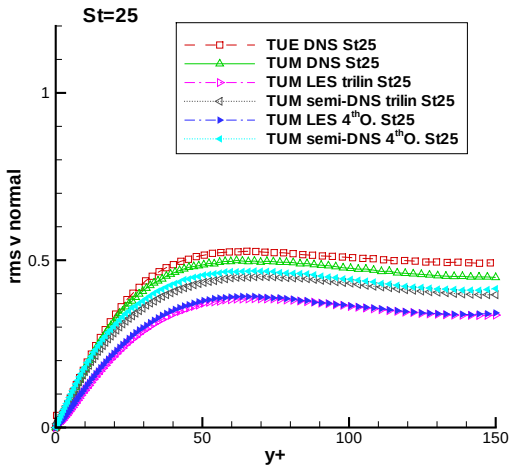

Figure 27: rms of particle wall-normal velocity fluctuations, $St = 25$

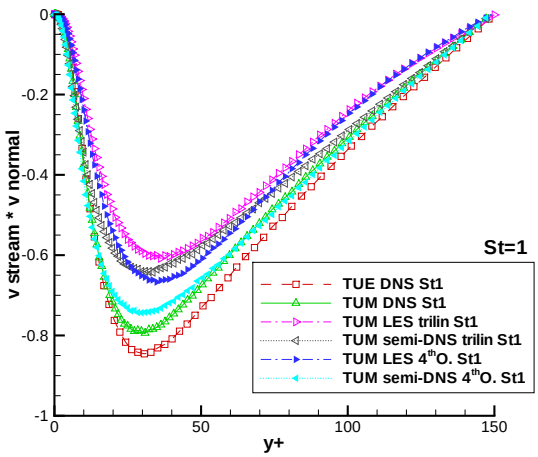

Figure 28: particle Reynolds stresses, streamwise/wall-normal component, $St = 1$

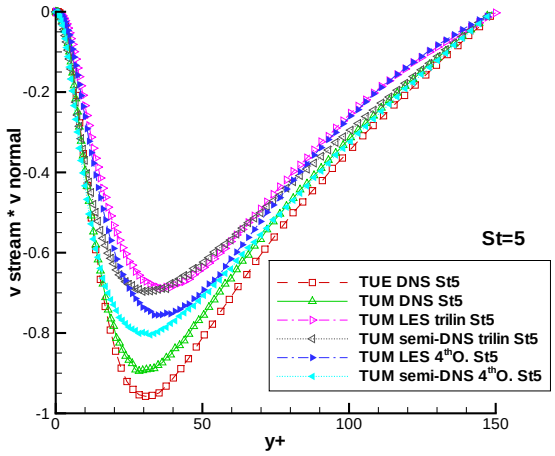

Figure 29: particle Reynolds stresses, streamwise/wall-normal component, $St = 5$

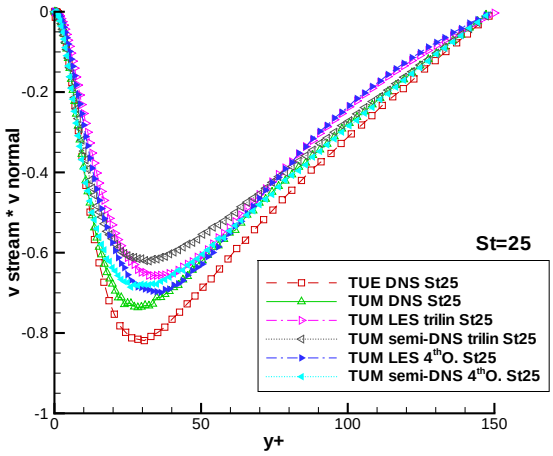

Figure 30: particle Reynolds stresses, streamwise/wall-normal component, $St = 25$

5 Index of figures / data

Figure	file	data columns
2	dns_results, finedns_results, les_results, semidns_results	1,2
3	dns_results, finedns_results, les_results, semidns_results	1,4
4	dns_results, finedns_results, les_results, semidns_results	1,6
5	dns_results, finedns_results, les_results, semidns_results	1,5
6	dns_results, finedns_results, les_results, semidns_results	1,10
7	dns_concentration_wall, les2_concentration_wall, semidns2_concentration_wall, les4_concentration_wall, semidns4_concentration_wall	1,2
8	dns_concentration_wall, les2_concentration_wall, semidns2_concentration_wall, les4_concentration_wall, semidns4_concentration_wall	1,3
9	dns_concentration_wall, les2_concentration_wall, semidns2_concentration_wall, les4_concentration_wall, semidns4_concentration_wall	1,4
10	dns_concentration_center, les2_concentration_center, semidns2_concentration_center, les4_concentration_center, semidns4_concentration_center	1,2
11	dns_concentration_center, les2_concentration_center, semidns2_concentration_center, les4_concentration_center, semidns4_concentration_center	1,3
12	dns_concentration_center, les2_concentration_center, semidns2_concentration_center, les4_concentration_center, semidns4_concentration_center	1,4
13	dns_concentration, les2_concentration, semidns2_concentration, les4_concentration, semidns4_concentration	1,62
14	dns_concentration, les2_concentration, semidns2_concentration, les4_concentration, semidns4_concentration	1,63
15	dns_concentration, les2_concentration, semidns2_concentration, les4_concentration, semidns4_concentration	1,64
16	dns_particles_1, les2_particles_1, semidns2_particles_1, les4_particles_1, semidns4_particles_1	1,3
17	dns_particles_5, les2_particles_5, semidns2_particles_5, les4_particles_5, semidns4_particles_5	1,3
18	dns_particles_25, les2_particles_25, semidns2_particles_25, les4_particles_25, semidns4_particles_25	1,3
19	dns_particles_1, les2_particles_1, semidns2_particles_1, les4_particles_1, semidns4_particles_1	1,6
20	dns_particles_5, les2_particles_5, semidns2_particles_5, les4_particles_5, semidns4_particles_5	1,6
21	dns_particles_25, les2_particles_25, semidns2_particles_25, les4_particles_25, semidns4_particles_25	1,6
22	dns_particles_1, les2_particles_1, semidns2_particles_1, les4_particles_1, semidns4_particles_1	1,8
23	dns_particles_5, les2_particles_5, semidns2_particles_5, les4_particles_5, semidns4_particles_5	1,8
24	dns_particles_25, les2_particles_25, semidns2_particles_25, les4_particles_25, semidns4_particles_25	1,8

Figure	file	data columns
25	dns_particles_1, les2_particles_1, semidns2_particles_1, les4_particles_1, semidns4_particles_1	1,7
26	dns_particles_5, les2_particles_5, semidns2_particles_5, les4_particles_5, semidns4_particles_5	1,7
27	dns_particles_25, les2_particles_25, semidns2_particles_25, les4_particles_25, semidns4_particles_25	1,7
28	dns_particles_1, les2_particles_1, semidns2_particles_1, les4_particles_1, semidns4_particles_1	1,10
29	dns_particles_5, les2_particles_5, semidns2_particles_5, les4_particles_5, semidns4_particles_5	1,10
30	dns_particles_25, les2_particles_25, semidns2_particles_25, les4_particles_25, semidns4_particles_25	1,10

References

[1] Marchioli, C., Soldati, A., Kuerten, J., Arcen, B., Taniere, A., Goldensoph, G., Squires, K., Cargnelutti, M. & Portela, L. 2008 Statistics of particle dispersion in direct numerical simulations of wall-bounded turbulence: Results of an international collaborative benchmark test. *Int. J. Multiphase Flow* **34**, 879–893.

[2] Meneveau, C., Lund, T. S. & Cabot, W. H. 1996 A Lagrangian dynamic subgrid-scale model of turbulence. *J. Fluid Mech.* **319**, 353–385.